Rev. Mexicana Astron. Astrof. **12**, 143-152 (1986)

MAGNETOHYDRODYNAMIC EFFECTS IN RADIO JETS

Elisabete M. de Gouveia Dal Pino[1] and Reuven Opher[2]

Instituto Astronômico e Geofísico, USP, Brasil

ABSTRACT. Radio jets from active galactic nuclei and QSO's are characterized by: 1) a high degree of polarization; 2) highly organized magnetic fields which are frequently parallel to the jet axis near the nucleus, becoming approximately perpendicular in the region where the jet becomes more highly collimated; and 3) slow and rapid changes of opening angle. In view of these observational facts, we study the dynamic effects of magnetic fields on jets. For a quantitative analysis of the problem, we consider a continuous jet with negligible viscous and thermal conductive effects and infinite electrical conductivity.We show that solutions of the magnetohydrodynamic equations give a natural explanation for the observed slow and rapid changes of opening angle.We show also that the observed opening angle and its rate of change put limits on the possible physical parameters of the jet .

I. INTRODUCTION

Key words: radio jets, active galactic nuclei

Highly sensitive VLA observations of the radio jets emanating from the galactic nucleus to the lobes of the extended extragalactic radio sources 3C 449 and 3C 296 (Perley et al. 1979; Birkinshaw et al. 1981) , NGC 315 (Bridle et al. 1979; Willis et al. 1981), 3C 31 (Fomalont et al. 1980; Bridle et al. 1980), M87 (Owen et al. 1980; Biretta et al. 1983) and NGC 5128 (CenA) (Burns et al. 1983; Brodie et al. 1983), have revealed important characteristics about the structure of these objects. The jets are well collimated (frequently with an angular opening $2\theta \leq 20^{o}$) . Their opening angle is not constant but varies with increasing distance from the radio core such as is the case for the jets in NGC 315 and 3C 31 which exhibit an initial regime of rapid transverse expansion, followed by regimes of lateral confinement and then apparently free expansion. Polarization data suggest that the magnetic field configuration in jets is highly ordered and its dominant component, usually predominantly parallel to the jet axis near the nucleus, becomes approximately perpendicular at greater distances. In particular, the jets in NGC 315, 3C 449, 3C 296 and 3C 31 have this change in magnetic field direction in the region where the jet becomes more highly collimated and more symmetric in intensity (Fomalont et al. 1980; Lupton and Gott III, 1982).

As remarked by Bicknell and Henriksen (1980, hereafter BH) and Chan and Henriksen

1. Work supported by FAPESP 2. Work partially supported by CNPq

(1980,hereafter CH) these observational facts suggest that the well-ordered magnetic fields in jets, although apparently weak ($\sim 10^{-4}$ - 10^{-6}G, as estimated from minimum energy considerations; Perola 1981), may have an important role in the observed variations of jet transverse expansion. However, most of the models proposed to explain the radio sources and in particular, the jet collimation (e.g. Eichler 1982, Siah and Wiita 1983, and references therein) ignore the dynamical effects of magnetic fields in the plasma flow. In these hydrodynamical models, collimation is imposed only by a confining gas cloud. (CH) and (BH), on the other hand, include the magnetic field in the dynamics of jets and show that it can produce additional collimation.

In this work we investigate the conditions which can produce the observed changes in opening angle of radio jets with distance from the nucleus ($\partial\theta/\partial z$). To achieve this aim, the external pressure and the magnetic field of the jet are taken into account in order to correctly reproduce the dynamical behaviour of the jet. Thus, using a complete set of magnetohydrodynamic (MHD) equations, we show that solutions of these equations may reproduce the observed changes in opening angle of jets. We apply our calculations to the NGC 315 main jet, using the best existing data for it, and show that the changes in opening angle impose limits on the possible values of the physical parameters of the jet.

In section II we discuss the magnetohydrodynamic equation used in analysing radio jets. In section III we discuss the rate of change of the opening angle and define a characteristic collimation length for jets. Finally, in section IV, we apply the analysis to some observational data on the main jet of NGC 315.

II. THE MAGNETOHYDRODYNAMIC EQUATIONS

We assume that a continuous and stationary jet of thermal plasma and relativistic particles is flowing to the radio lobes of the radio sources and that such a flow is partially confined and collimated by external pressure. Polarization measurements and a number of theoretical considerations give some evidence that the jets have, in general, relatively large plasma densities ($\sim 10^{-2}$ - 10^{-4}cm^{-3}) and flow velocities $\gtrsim 10^{8}$ cm/s (Perley et al. 1979; Biretta et al. 1983; Burns et al. 1983; Fomalont et al. 1980; Willis et al. 1981). If in addition to these features we neglect viscous and thermal conductivity effects, but consider infinite electrical conductivity and include the dynamical effects of the magnetic field, the flow can be described by the non-relativistic, stationary, axisymmetric and adiabatic MHD equations given, in cylindrical coordinates (R; ϕ, z) by (see Heinemann and Olbert, 1980 hereafter HO).

$$a\,\frac{\partial^2\Psi}{\partial R^2} + 2b\,\frac{\partial^2\Psi}{\partial R\partial z} + c\,\frac{\partial^2\Psi}{\partial z^2} + d = 0 \qquad (1)$$

$$\vec{B}_p = \frac{1}{R}\left(\frac{\partial\Psi}{\partial R}\,\hat{z} - \frac{\partial\Psi}{\partial z}\,\hat{R}\right) \qquad (2) \qquad \vec{v}_p = \frac{1}{\alpha\rho}\,\vec{B}_p \qquad (3)$$

$$\omega = (\alpha\rho v_\phi - B_\phi)/\alpha\rho R \qquad (4) \qquad L = R\,(v_\phi - \alpha B_\phi/4\pi) \qquad (5)$$

$$E = \frac{1}{2}\,v^2 + W + \Phi - \omega R v_\phi \qquad (6)$$

where ρ is the mass density; $\vec{v}_p = v_R \hat{R} + v_z \hat{z}$ and v_ϕ are, respectively, the poloidal and the azimuthal components of the velocity $\vec{v}$; $\vec{B}_p = B_R \hat{R} + B_z \hat{z}$ and B_ϕ are the poloidal and the azimuthal components of the magnetic field $\vec{B}$; Ψ is the magnetic stream function and α, ω (the total angular velocity), L (the total angular momentum per unit mass) and E (the total energy per unit mass) are field and stream line constants. In the energy Eq. (6), W is the enthalpy per unit mass and Φ is the external gravitational potential. In this work, since we are analysing the transverse variations of jets at considerable distances from the nucleus, we neglect gravitational effects. The coefficients a, b, c and d in Eq. (1) are (neglecting gravitational effects) functions of R, z, $\vec{\nabla}\Psi$, α, ω, L, E, and s (the entropy per unit mass of the gas and also a stream and field line constant), as well as the derivatives of these field (and stream) line constants with respect to Ψ: α', ω', L', E' and s'. According to Eq. (2), α', for example, is given by

$$\alpha' = - \frac{\partial \alpha}{\partial z} / (R\, B_R) = \frac{\partial \alpha}{\partial R} / (R\, Bz) \tag{7}$$

and similar expressions are also valid for ω', L', E' and s'. The complete relations for the coefficients a, b, c and d are given by (HO) in Eqs. (22) - (27) of their paper.

An equation of state is required to complete the above system (Eqs. 1 - 6). Thus, considering a polytropic pressure relation

$$p = A\, \rho^{\gamma},$$

where A is a function of s and γ is the polytropic index, and assuming that the beam thermal gas is ideal ($p \propto \rho T$) and s is constant throughout the jet (isentropic fuid), we have

$$p = p_c \left(\frac{\rho}{\rho_c}\right)^{\gamma} \tag{8}$$

with $\gamma = 5/3$ and p_c and ρ_c, the central values of the pressure and density, respectively. It can be noted that with the above assumption, the last term in Eq. (26) of (HO) vanishes and according to (8), the enthalpy $W = \int dp/\rho$ in Eq. (6)(where the integration is taken along a field line) is given by

$$W = \frac{c_s^2}{\gamma - 1} \tag{9}$$

where c_s is the sound speed

$$c_s^2 = (\partial p/\partial \rho)s \tag{10}$$

III. THE RATE OF CHANGE OF OPENING ANGLE $\dot{\theta}$ AND THE CHARACTERISTIC COLLIMATION LENGTH λ_c

In order to quantitatively describe the opening angle variations in radio jets with the distance from the nucleus, we define a characteristic collimation length for the jet

$$\lambda_c \equiv \frac{-\pi}{2} \left[\frac{B_R}{\partial B_R/\partial z}\right]_{R_o} \tag{11}$$

all quantities being evaluated at the edge of the jet R_o. From Eqs. (1), (2) and (11) :

$$\frac{\lambda_c}{R_o} = \frac{\pi}{2}\left\{B_R\, c\left[a\frac{\partial}{\partial R}(R\,B_z) - 2b\frac{\partial}{\partial R}(R\,B_R) + d\right]^{-1}\right\}_{R_o} \tag{12}$$

From Eq. (3) we have

$$\left[\tan\theta\right]_{R_o} = \left[v_R/v_z\right]_{R_o} = \left[B_R/B_z\right]_{R_o} \tag{13}$$

where $\theta(R_o)$ is the half opening angle at R_o. This relation leads to

$$\left[\partial v_R/\partial z\right]_{R_o} = \left[\frac{v_z}{\cos^2\theta}(\partial\theta/\partial z) + \tan\theta\,(\partial v_z/\partial z)\right]_{R_o} \tag{14}$$

$$\left[\partial B_R/\partial z\right]_{R_o} = \left[\frac{B_z}{\cos^2\theta}(\partial\theta/\partial z) + \tan\theta\,(\partial B_z/\partial z)\right]_{R_o} \tag{15}$$

We suppose that tan θ is small (an approximation generally valid for radio jets) and also that $\partial v_z/\partial z$ and $\partial B_z/\partial z$ are small, so we have in Eqs. (14) and (15):

$$\left|\tan\theta\,\frac{\partial v_z}{\partial z}\right| << \left|\frac{v_z}{\cos^2\theta}\,\frac{\partial\theta}{\partial z}\right| \tag{16}$$

$$\left|\tan\theta\,\frac{\partial B_z}{\partial z}\right| << \left|\frac{B_z}{\cos^2\theta}\,\frac{\partial\theta}{\partial z}\right| \tag{17}$$

The expected smallness of $\partial v_z/\partial z$, for example, is a result of the approximate constancy of v_z (BH). From Eqs. (13) - (17) and (11) we then have

$$\left[\frac{1}{B_R}\frac{\partial B_R}{\partial z}\right]_{R_o} = \left[\frac{\cos^{-2}\theta}{\tan\theta}\,\frac{\partial\theta}{\partial z}\right]_{R_o} = \left[\frac{1}{v_R}\,\frac{\partial v_R}{\partial z}\right]_{R_o} = -\frac{\pi}{2\,\lambda_c} \tag{18}$$

This relation offers a simple manner of estimating λ_c directly from the observations, since the change in opening angle of the jet with distance from the nucleus $\partial\theta/\partial z$, as well as θ, are measurable quantities. The relation among v_R, θ and λ_c at the edge of the jet R_o, is shown in Fig. 1.

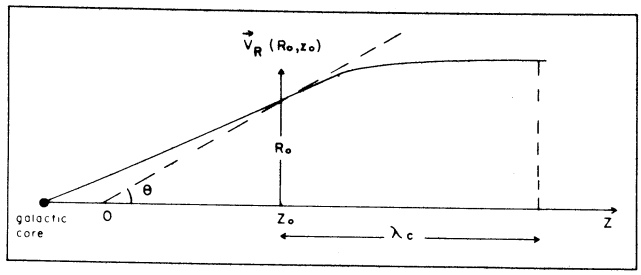

Fig. 1 - The relation among v_R, $\theta = \tan^{-1}(v_R/v_z)$ and λ_c at the boundary point (R_o,z_o) of the jet. The distance z is measured along the axis of the jet and z_o is given by $z_o = R_o/\tan\theta$. λ_c gives the approximate distance from the point (R_o, z_o) where v_R and θ vanish.

We note from Eq. (18) that a positive value of λ_c, for positive values of θ, corresponds to a decrease of the radial boundary velocity v_R as a function of z and thus, to an

ncrease in jet collimation, as can be seen in Fig. 1. For this reason, we call λ_c the collimation length of the jet. If v_R had a harmonic dependence, for example, $v_R = v_R(R_o, z_o) \times \{1 - \sin [2\pi/\lambda\ (z - z_o)]\}$, we would identify λ_c in Eq. (18) and in Fig. 1 as $\lambda/4$ and thus λ_c would give the distance in which v_R vanishes from the point (R_o, z_o), causing the decrease in the jet opening angle. In the opposite case, i.e., for negative values of λ_c (and positive θ) we clearly have an increase in the jet opening angle.

The collimation of the jet is proportional to the rate of change of the opening angle with distance. We thus define, using Eq. (18)

$$\dot{\theta} \equiv R_o \left[\frac{\partial\theta}{\partial z}\right]_{R_o} = -\frac{\pi}{2}\ \frac{\cos^2\theta\ \tan\theta}{(\lambda_c/R_o)} \tag{19}$$

and the relation of λ_c/R_o and $\dot{\theta}$ is

$$\frac{\lambda_c}{R_o} = -\frac{\pi}{2}\ \frac{\cos^2\theta\ \tan\theta}{\dot{\theta}} \tag{20}$$

To construct the solution of Eq. (12) at z_o some assumptions are required. As can be seen in Eqs. (3) - (12) and Eq. (26) of(HO)not only ρ, p, $\vec{v}$ and $\vec{B}$ must be known as functions of R, but also their radial derivatives. As a rough attempt of reproducing the real physical conditions in the beam, we impose gaussian behaviour at z_o on ρ (R), $B_p(R)^2$,$(B_\phi(R)/R)^2$ and $v_\phi(R)/R)^2$ of the type:

$$g(r) = g_c\ e^{-R^2/H^2} \tag{21}$$

with

$$H^2 = R_o^2/\ln(g_c/g_o). \tag{22}$$

where g_c and g_o are, respectively, the values of the physical quantity g(R) at the center and at the boundary of the beam at z_o, and H is the scale factor that we assume to be the same for all the gaussian functions. From Eqs. (13) and (21) we can then calculate B_z and B_R:

$$B_z = B_p \cos\theta \tag{23}$$

$$B_R = B_z \tan\theta \tag{24}$$

We assume that discontinuity effects in the total pressure at the edge of the flow are negligible as compared with the other forces involved, thus imposing the pressure equilibrium condition at the boundary point (R_o, z_o):

$$p_e = p_o + (B_{p_o}^2 + B_{\phi_o}^2)/8\pi \tag{25}$$

and employing Eqs. (8), (22), (23) and (24), we then derive an expression for B_{ϕ_o}

$$B_{\phi_o}^2 = (p_e - p_c\ K_\rho^\gamma)\ 8\pi - B_{z_c}^2\ K_\rho \tag{26}$$

with

$$K_\rho = \rho_o/\rho_c \ , \tag{27}$$

where the quantities with subscripts "c" and "o" are the values at z_o of the associated quantities at the center and at the edge R_o, respectively, and p_e is the external thermal pressure. We assume here that magnetic pressure in the jet is much greater than the external magnetic pressure.

We have for the axial component of the flow velocity

$$v_z = M_z \, c_s \tag{28}$$

where c_s is given by Eq. (10) and M_z is the axial Mach number. The radial component is then calculated in a similar manner as B_R (Eq. 24).

In Eq. (26) $B_{\phi_o}^2$ must be positive. This imposes a restriction on $K_p = p_e/p_c$

$$K_p \geq K_\rho^\gamma + \frac{\gamma}{2} \frac{M_z^2}{M_{Az_c}^2} K_\rho \tag{29}$$

where M_{Az_c} is the axial Alfvēnic Mach number at the center of the beam

$$M_{Az_c}^2 = v_{z_c}^2 / (B_{z_c}^2 / 4\pi\rho_c) \tag{30}$$

In the regions of the beam we are considering, this ratio must be greater than unity since the opposite condition would imply a large poloidal magnetic pressure that would disperse the flow (BH).

The non-relativistic condition, $v << c$, also imposes a limit on the physical parameters of the jet. This condition and Eqs. (10), (8), (13), (22) and (28) imply that at (R_o, z_o)

$$K_{v_\phi}^2 = \left(\frac{v_\phi}{v_z}\right)_{R_o}^2 << \frac{c^2}{\gamma} \frac{\rho_c}{p_e} \frac{K_p}{M_z^2} \frac{1}{K_\rho^{\gamma-1}} - \frac{1}{\cos^2\theta} \tag{31}$$

It is to be noted that neglecting gravitational effects, λ_c/R_o in Eq. (12) (and thus also $\dot{\theta}$, Eq. 19) is independent of the sign of θ. In fact, from Eq. (23) of (HO)

$$b = v_p^2 \, v_z^2 \tan\theta$$

and from Eqs. (13) and (21)

$$\left[\partial (R B_R)/\partial R\right]_{R_o} = \left[B_z \tan\theta \, (1 - 2R_o/H^2)\right]_{R_o} \ ,$$

we see that $2b \, [\partial(R B_R)/\partial R]$, the only term in Eq. (12) where the sign of θ enters, is independent of its sign.

Using the formulation described above (Eqs. 12 - 31), $\dot{\theta}$ and λ_c/R_o (as defined by Eqs. (19) and (12), respectively) can be calculated as a function of the beam parameters θ, K_ρ, K_p, M_z, M_{Az_c} and $K_{v\phi}$ and then compared with the observed values for a given jet. However, since these beam parameters are not known or roughly estimated from observational data, we construct by numerical calculations curves of $\dot{\theta}$ and λ_c/R_o as a function of these beam parameters in order to investigate appropriate values for them.

IV. APPLICATION TO THE MAIN JET OF NGC 315

The observed half opening angle variations of the main jet of NGC 315, as a function of the distance from the nucleus (in units of arc sec) found by Willis et al. (1981), is shown in Fig. 2. We note the strong collimation between the distances 120" to 420" from the nucleus where θ changes from $+4.9^o$ to -2.3^o, followed by the sudden large positive change of opening angle at 420", and then the region > 420" of constant transverse expansion with $\theta=+4.9^o$.

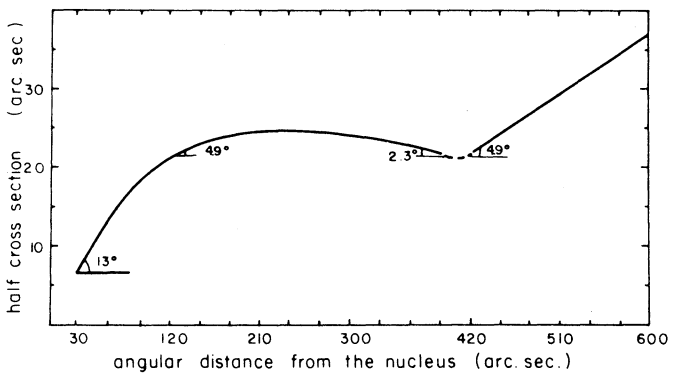

Fig. 2. The observed half-width and opening angle variations as a function of distance from the galactic nucleus for the main jet of NGC 315 (Willis et al. 1981).

We restrict our analysis in the present paper to the transition region near 420". Table 1 lists the observed parameters near this point. Columns 1, 2, 3 and 4 give, respectively, the angular distance (d), the half cross-sectional width (R_o), the half opening angle (θ) and $\tan\theta = \left[\overline{v_R/v_z}\right]R_o$ (Willis et al. 1981). Columns 5 and 6 give, respectively, the values of $\dot{\theta}$ and λ_c/R_o (Eqs. 19 and 20) obtained from the observed quantities in columns 1-4. We note, in particular, the transition from collimation ($\dot{\theta}=-0.42$) at d = 390", large acceleration ($\dot{\theta}=+5.2$) at d = 420", and free expansion ($\dot{\theta}=0$) at d = 450".

Figs. 3 and 4 show some results of our calculations for $\theta = 4.9^o$. Fig. 3 gives curves of $\dot{\theta}$ and λ_c/R_o as a function of the beam parameter $K_p = p_e/p_c$, for different values of K_ρ (Eq. 27). For each curve, the lower limit of K_p is fixed by Eq. (29). In all curves, the values of the other beam parameters are fixed at $M_z = 12$, $M_{Az_c} = 16$ and $K_{v\phi} = 0$. This estimate for M_z (Eq. 28) was obtained by assuming $M_z \simeq 1/\tan\theta$ (this condition is strictly valid only if the jet is expanding freely; for a thermally confined jet this estimate is a minimum). The value

TABLE 1. Observed expansion parameters of the main jet of NGC 315 near 420" (Willis et al. 1981)

d(arc sec)	R_o(arc sec)	θ^o	$\tan\theta = \left[\frac{\bar{v}_R}{\bar{v}_z}\right]_{R_o}$	$\dot{\theta}$	λ_c/R_o
330	23.5	-1.43	-0.025	-0.09	24.5
360	23	-1.72	-0.030	-0.22	12.1
390	21.5	-2.3	-0.040	-0.42	8.7
420	21.5	4.9	0.085	5.2	-1.5
450	24.5	4.9	0.085	0	-

of M_{Az_c} (Eq. 30) was obtained from $M_z = 12$ and taking $\rho_c \simeq 10^{-4}$ cm^{-3}, $B_{z_c} \simeq 1.7\times10^{-6}$ G and $c_{sc} \simeq 5\times10^7$ cm/s, the latter values being derived from polarization data and from conditions of equipartition of energy found by Willis et al. (1981). In Fig. 3, we have no rotation of the plasma jet ($K_{v\phi}$=0) (Eq. 31). We see from Fig. 3. that only values in the narrow range of $0.10 \lesssim K_\rho \lesssim 0.12$ are appropriate in order to reproduce the observed value of $\dot{\theta} \sim 5.2$ and $\lambda_c/R_o \sim -1.5$ at the region 420". For the curve of $K_\rho = 0.10$, these values of $\dot{\theta}$ and λ_c/R_o are obtained for $K_p \lesssim 0.3$ and for the curve of $K_\rho = 0.12$, these values are obtained for $K_p \gtrsim 0.6$ (see Fig. 3a).

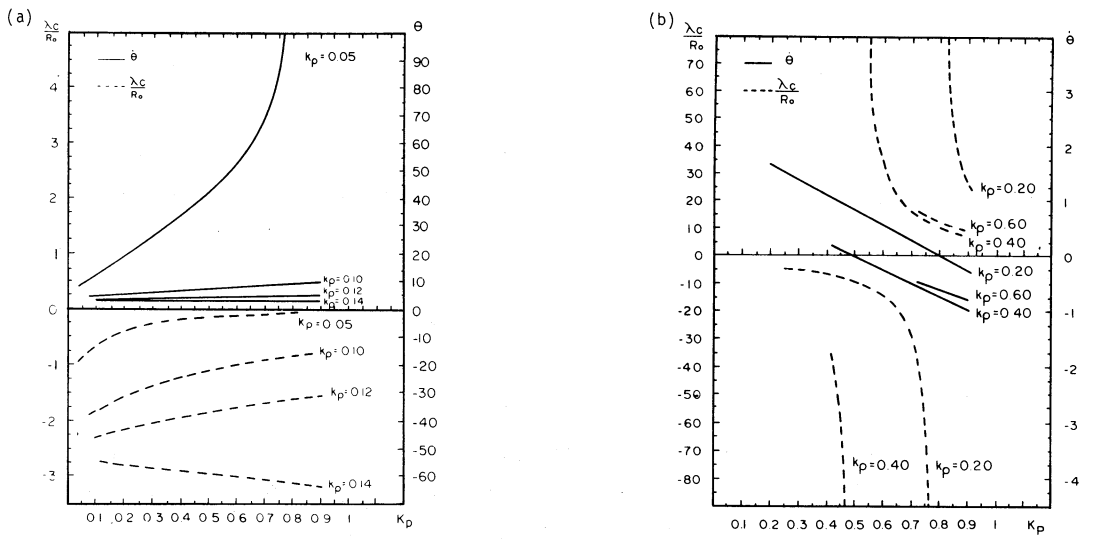

Fig. 3 - The rate of change of opening angle $\dot{\theta}$ and the collimation length λ_c versus $K_p = p_e/p_c$ for different values of $K_\rho = \rho_o/\rho_c$, with $\theta = 4.9^o$, $M_z = 12$, $M_{Az_c} = 16$ and $K_{v\phi} = 0$. In Fig. 3a we have $K_\rho = 0.05$, 0.10, 0.12 and 0.14, and in Fig. 3b we have $K_\rho \cong 0.2$, 0.4 and 0.6. Note the expanded scale of $\dot{\theta}$ in Fig. 3b as compared with Fig. 3a.

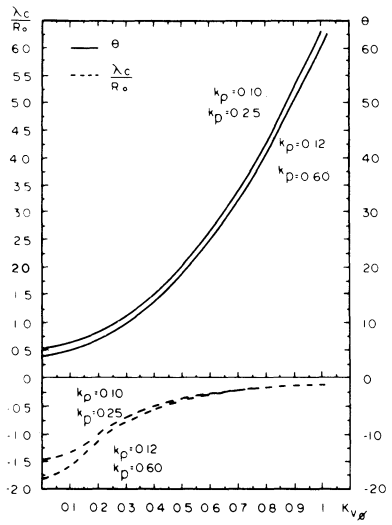

Fig. 4 - $\dot{\theta}$ and λ_c/R_o versus $K_{v\phi}$ for $K_\rho = 0.10$ and $K_p = 0.25$, and for $K_\rho = 0.12$ and $K_p = 0.60$, with the other beam parameters fixed at $\theta = 4.9^o$, $M_z = 12$ and $M_{Az_c} = 16$.

Figure 4 shows what happens when rotation exists. In this figure we have the curves of $\dot{\theta}$ and λ_c/R_o as a function of $K_{v\phi}$ for the pairs of values of K_ρ and K_p: ($K_\rho = 0.10$, $K_p = 0.25$) and ($K_\rho = 0.12$, $K_p = 0.60$) with the other beam parameters fixed at the values previously given. We note that an increase in $K_{v\phi}$ (and thus in the angular velocity of the plasma about the axis of rotation) implies, as expected, an increase in $\dot{\theta}$.

Figures 3a and 3b also reveal other interesting results. We see that for small values of $K_\rho (< 0.20)$ and thus for large gradients of thermal pressure ∇p (according to Eq. 8), we have $\dot{\theta}$ always positive ($\lambda_o/R_o < 0$) that is, only increasing jet transverse expansion occurs for any value of K_p. However, for greater values of K_ρ and thus smaller values of ∇p, collimation ($\dot{\theta} < 0$, $\lambda_c/R_o > 0$) may take place (see Fig. 3b). For $K_\rho = 0.20$, for example, the transition from increasing jet transverse expansion to collimation occurs at $K_p = 0.8$. On the other hand, for $K_\rho = 0.60$ there is only collimation.

We might expect that for a fixed value of K_p an increase in K_ρ causes a decrease in $\dot{\theta}$ (or in λ_c/R_o) as a consequence of the decrease in ∇p. This is not verified, however, for $K_\rho \geq 0.40$, as can be seen in Fig. 3b, where $\dot{\theta}(K_\rho = 0.60) > \dot{\theta}(K_\rho = 0.40)$ for any K_p. This effect is caused by the increase in the magnetic pressure ($B^2/8\pi$). In fact, for large values of K_ρ, as K_ρ grows we have at the same time an increase in the total magnetic pressure (caused by the increase in $\vec{B}_p$, even though B_ϕ decreases; see Eqs. 21, 22 and 26) and a decrease in ∇p. While the decrease in ∇p tends to decrease $\dot{\theta}$, the increase in the magnetic pressure tends to increase $\dot{\theta}$. Since ∇p is small for large values of K_ρ, the increase in the magnetic pressure dominates in these cases.

It can be noted also from Fig. 3 that for a fixed value of K_ρ with $K_\rho \geq 0.14$, $\dot{\theta}$ (and λ_c/R_o) decreases with increasing K_p, but the opposite occurs for $K_\rho < 0.14$. This result is due to the dispute between two different effects caused by the increase in the azimuthal component of the magnetic field (B_ϕ), when K_p grows (see Eq. 26). One of these effects is the increase of the dynamical effect of B_ϕ, which according to Eqs. (3) and (4) acts to decrease the angular momentum

of the plasma about the axis of rotation and thus to increase the collimation and the other one is the increase of the total magnetic pressure. Accordingly, for the curves in Fig. 3 with $K_\rho \geq 0.14$, the dynamical effect of B_ϕ dominates causing the decrease in $\dot{\theta}$, while for the curves with $K_\rho < 0.14$ the magnetic pressure dominates causing the increase in $\dot{\theta}$ as K_p grows.

We confined the present discussion to the region of 420" of the main jet of NGC 315. A more complete analysis of the various physical parameters on $\dot{\theta}$ (and λ_c/R_o) applied to the available data on radio jets will be published elsewhere.

Acknowledgements. We would like to thank Luiz C. Jafelice, Vera J.S. Pereira, José C.N. Araújo, João B.G. Canalle and Arnaldo Dal Pino Jr. for useful comments.

REFERENCES

Bicknell, G.V. and Henriksen, R.N. 1980, Astroph. Lett., 21, 29 .
Biretta, J.A., Owen, F.N. and Hardee, P.E. 1983, Ap. J., in press .
Birkinshaw, M., Laing, R.A. and Peacock, J.A. 1981, M.N.R.A.S., 197, 253.
Bridle, A.H., Davis, M.M., Fomalont, E.B., Willis, A.G. and Strom, R.G. 1979, Ap. J., 228, L9.
Bridle, A.H., Henriksen, R.N., Chan, K.L., Fomalont, E.B., Willis, A.G. and Perley, R.A. 1980, Ap. J., 241, L145.
Brodie, J., Königl, A. and Bowyer, S. 1983, Ap. J., 273, 154 .
Burns, J.O., Feigelson, E.D. and Schreier, E.J. 1983, Ap. J., 273, 128 .
Chan, K.L. and Henriksen, R.N., Ap. J., 241, 534 .
Eichler, D. 1982, Ap. J., 263, 571 .
Fomalont, E.B., Bridle, A.H., Willis, A.G. and Perley, R.A. 1980, Ap. J., 237, 418 .
Heinemann, M. and Olbert, S. 1978, J. Geophys. Res., 83, 2457 .
Lupton, R.H. and Gott III, J.R. 1982, Ap. J., 255, 408 .
Owen, F.N., Hardee, P.E. and Bignell, R.C. 1980, Ap. J. 239, L11 .
Perola, G.C. 1981, Fundam. Cosmic Ph., 7, 59.
Perley, R.A., Willis, A.G. and Scott, J.S. 1979, Nature, 281, 437.
Siah, M.J. and Wiita, P. 1983, Ap. J., 270, 427 .
Willis, A.G., Strom, R.G., Bridle, A.H. and Fomalont, E.B. 1981, A.A., 95, 250 .

Elisabete M. de Gouveia Dal Pino and Reuven Opher: Instituto Astrônomico e Geofísico, Universidade de São Paulo, Caixa Postal 30627, CEP 01051, São Paulo, SP,Brasil.